ELSEVIER

S0032-3861(96)00230-3

Polymer Vol. 37 No. 17, pp. 3937–3943, 1996

0032-3861/96/$15.00 + 0.00

Study of semicrystalline–amorphous diblock copolymers: 1. Microphase separation, glass transition and crystallization of tetrahydrofuran–methyl methacrylate diblock copolymers

Lizhi Liu*, Bingzheng Jiang and Enle Zhou

Polymer Physics Laboratory, Changchun Institute of Applied Chemistry, Chinese Academy of Sciences, Changchun 130022, People's Republic of China

(Received 29 June 1994; revised 19 December 1994)

The microphase separation, glass transition and crystallization of two series of tetrahydrofuran–methyl methacrylate diblock copolymers (PTHF-*b*-PMMA), one with a given PTHF block of $\bar{M}_n = 5100$ and the other with a given PTHF block of $\bar{M}_n = 7000$, were studied in this present work. In the case of solution-cast materials, the microphase separation of the copolymer takes place first, with crystallization then gradually starting in the formed PTHF microphase. The T_g of the PMMA microphase shows a strong dependence on the molecular weight of the PMMA block, while the T_g of the PTHF microphase shows a strong dependence on the copolymer composition. The non-isothermal crystallization temperature (T_c) of the diblock copolymer decreases rapidly and continuously with the increase in the amorphous PMMA weight fraction; the lowest T_c of the copolymer is ca. 35 K lower than the T_c of the PTHF homopolymer. There also exists a T_c dependence on the molecular weight of the PTHF block. In addition, when the major component of the copolymer is PMMA, a strong dependence of the crystallizability of the copolymer on the molecular weight of the PTHF block is observed; the higher the molecular weight, then the stronger its crystallizability. The melting temperature of the block copolymer is dependent on the copolymer composition and the molecular weight of its crystallizable block. Copyright © 1996 Elsevier Science Ltd.

(Keywords: block copolymer; phase separation; crystallization)

INTRODUCTION

The microphase separation of amorphous block copolymers has been extensively studied both theoretically[1–8] and experimentally[9–16]. The study of semicrystalline–amorphous block copolymers have also received some attention, especially in recent years, and a number of experimental investigations[17–36] and a few theoretical studies[37–39] have been carried out. The microphase separation behaviour of semicrystalline block copolymers is usually very different from that of amorphous block copolymers due to the added effect of crystallization of the crystallizable block[33]; the crystallization behaviour of this kind of copolymer is also different from its corresponding homopolymer blends and its corresponding semicrystalline homopolymer, because the crystallizable block is linked with an amorphous block through a covalent bond and the two blocks are usually incompatible, which could thus lead to microphase separation.

Such semicrystalline copolymers have many aggregated structures in solution; the lamellar liquid crystalline structures of ethylene oxide–styrene diblock copolymer (PEO-*b*-PS) and ethylene oxide–butadiene (PEO-*b*-PB) diblock copolymers have been studied by Gervais and Gallot[17–20]. Very recently, the very special crystalline aggregates of PEO-*b*-PS diblock copolymer, when grown from solution, was reported by Gast *et al.*[21] In the case of solution casting, the crystalline morphology of this kind of copolymer usually shows a strong dependence on the casting solvent[23,32], due to the effect of the solvent on its microphase separation. The melt crystallization behaviour of the copolymer is also very different from that of semicrystalline homopolymers; the kinetics (e.g. of thermal annealing) plays a very important role in crystallizable homopolymers[40] and a less important role in crystallizable block copolymers[37]. The nucleation behaviour of some semicrystalline–amorphous block copolymers could also be somewhat unusual, and both heterogeneous and homogeneous nucleation could be observed in the same crystallization process[22]. In recent years, a few further studies on the crystalline structure of semicrystalline–amorphous block copolymers have been carried out by Cohen and coworkers[28–30,33] and by Nojima *et al.*[31]. Douzinar and Cohen[30] studied chain folding in ethylene-*co*-butylene-*b*-ethylethylene (EBEE) semicrystalline diblock copolymers by X-ray pole-figure

* To whom correspondence should be addressed. Present address: Department of Chemistry, State University of New York at Stony Brook, Stony Brook, NY 11794-3400, USA

analysis and small-angle X-ray scattering techniques. Nojima *et al.*[31] studied ϵ-caprolactone–butadiene diblock copolymers (PCL-*b*-PB) by small-angle X-ray scattering (SAXS) at various temperatures; the morphology formation process was observed by time-resolved SAXS employing synchrotron radiation.

In this present paper, we report on the microphase separation, glass transition and crystallization of two series of tetrahydrofuran–methyl methacrylate diblock copolymers (PTHF-*b*-PMMA); one series of samples has a fixed PTHF block with $\bar{M}_n = 5100$ but different compositions, while the other series of copolymers has a fixed PTHF block with $\bar{M}_n = 7000$, and also with different compositions. The microphase separation and crystallization of our copolymers did not proceed simultaneously during solution casting; the microphase separation started well in advance of the crystallization, which was confirmed by small-angle X-ray scattering (SAXS) and wide-angle X-ray diffraction (WAXD) studies. The glass transition temperature (T_g) dependence of the PTHF microphase on the copolymer composition was different from the results reported for the glass transition behaviour of the PTHF microphase of PTHF/PS di- or triblock copolymers[24]. Different crystallization features of PTHF-*b*-PMMA diblock copolymers with PEO/PS di- or triblock copolymers, for which the final morphology was driven by the balance of microphase separation and crystallization in the case of solution casting, were also found and are discussed in this paper.

EXPERIMENTAL

Preparation of the copolymer

The PTHF-*b*-PMMA diblock copolymer was synthesized in our laboratory by a novel route which involved a cationic-to-anionic mechanism transformation. The PTHF prepolymers were synthesized by a cationic ring-opening mechanism. THF polymerization was initiated by adding benzyl bromide to a well-stirred solution of silver perchlorate hydrate in THF monomer at 258 K, and the reaction was allowed to proceed for about 40 h. This polymerization was finally terminated by the addition of aniline. The PTHF-*b*-PMMA diblock copolymer was obtained by adding sodium naphthalene to THF and a methyl methacrylate (MMA) monomer solution of the purified PTHF prepolymer. The copolymerization was allowed to proceed for ca. 16 h at room temperature and then terminated by pouring the reaction product into a solution of HCl in distilled water (0.1 mol l^{-1}). Purification of the block copolymer was carried out in order to remove the small amount of unwanted homopolymers. PTHF homopolymer was removed by precipitating the products three times from acetone solution into a large excess of petroleum ether; the homo-PMMA still remaining in the products was removed by crystallization of the PTHF block of the copolymer in acetone solution at 253 K.

Molecular characterization of polymers

The molecular weights of the two PTHF prepolymers were measured by membrane osmometry at 333 K in benzene (*Table 1*). The molecular weight of a PMMA-*b*-PTHF diblock copolymer was calculated from the molecular weight of its corresponding PTHF prepolymer and the copolymer composition determined by proton nuclear magnetic resonance (n.m.r.) spectroscopy, where 5% (wt/vol) solutions of polymer in deuterochloroform were examined. The diblock copolymers with a PTHF block of $\bar{M}_n = 7000$ are designated as H-, and the copolymer samples with a PTHF block of $\bar{M}_n = 5100$ are designated as L- (*Table 1*). In order to compare the crystallization behaviour of the PTHF-*b*-PMMA diblock copolymers with the PTHF/PMMA blends, a series of PTHF/PMMA blends with 10, 20, ..., and 90% PTHF were prepared by mixing in $CHCl_3$, and are designated as TM1, TM2, ..., and TM9, respectively. The number-average molecular weights of the PTHF and PMMA homopolymers that were used were 7000 and 20 000, respectively.

Table 1 Characterization of PTHF-*b*-PMMA diblock copolymers

Designation	$\bar{M}_n$ (g mol^{-1})	PTHF (wt%)	$\bar{M}_n$ of PTHF (g mol^{-1})
H-0	20 000	0	0
H-1	46 700	15	7000
H-2	29 200	24	7000
H-3	23 300	30	7000
H-4	20 000	35	7000
H-5	14 300	49	7000
H-6	12 300	57	7000
H-7	10 800	65	7000
H-8	7000	100	7000
L-1	24 300	21	5100
L-2	20 400	25	5100
L-3	17 000	30	5100
L-4	13 100	39	5100
L-5	12 400	41	5100
L-6	8400	61	5100
L-7	5100	100	5100

Differential scanning calorimetry (d.s.c.)

The PTHF-*b*-PMMA copolymer samples used for thermal analysis were solution-cast from a non-selective solvent, i.e. chloroform, and then dried under vacuum for 48 h at room temperature. All of the thermal analysis measurements were performed on a Perkin-Elmer DSC-2C differential scanning calorimeter. The glass transition temperatures (T_gs) of the PTHF and PMMA microphases of the copolymers were obtained during reheating at a rate of 20 K min^{-1} after the samples had been held at 383 K for 5 min and then cooled to 213 K at 20 K min^{-1}. The non-isothermal crystallization temperatures (T_cs) of the copolymers were obtained on cooling at 10 K min^{-1} from 383 K; the melting points and degrees of crystallinity of the copolymers were obtained from their thermograms after reheating at 10 K min^{-1} from 213 to 383 K.

SAXS and WAXD measurements

A Philips PW1700 automatic powder diffractometer with Ni-filtered CuKα radiation was used for the wide-angle X-ray diffraction (WAXD) measurements. The scans were obtained by using a 0.05° step programme with a collection time of 10 s per step. A Kratky small-angle X-ray scattering (SAXS) system with a proportional counter, attached to the above equipment, was used for obtaining the SAXS data of the copolymers. The numbers of pulses counted at each step was more than 10 000 in order to assure a standard deviation. The widths of the incident and receiving slits were 80 and 200 μm respectively.

RESULTS

An amorphous AB diblock copolymer microphase-separates when the incompatibility degree XN (where X is the Flory parameter characterizing the A–B interactions, and N is the polymerization index) of the two different blocks is above a critical value, which varies with copolymer composition f_A (i.e. $XN = 10.5$ for the symmetrical case where $f_A = 0.5$)[1]. This accounts for the variety of microphase-separation morphologies; i.e. spherical, cylindrical, lamellar, or ordered bicontinuous double-diamond (OBDD) microdomain forms, which can be obtained, depending on the copolymer composition. In order to achieve a good understanding of the microphase-separation and crystallization of the PTHF-*b*-PMMA diblock copolymers, the compatibility and crystallization behaviour of the PTHF/PMMA homopolymer blends were investigated first. Direct observations of the phase behaviour of PTHF/PMMA blend melts with an optical microscope showed that all of the blends from TM1 with 10% PTHF to TM9 with 90% PTHF were macroscopically incompatible. Therefore, a microphase-separated structure for our synthesized PTHF-*b*-PMMA diblock copolymers should be expected.

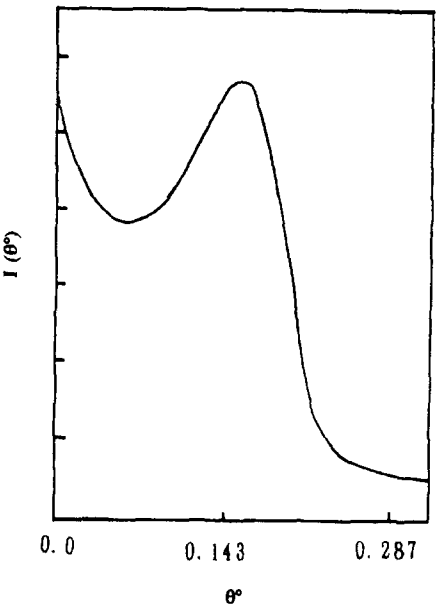

Figure 1 The SAXS curve of the PTHF-*b*-PMMA copolymer L-5 plotted as a function of the scattering angle Θ, measured immediately after it had been cast from $CHCl_3$

Separate processes of microphase separation and crystallization

Direct observation of the PTHF-*b*-PMMA copolymers at 383 K in an optical microscope showed that all of them were macroscopically homogeneous, indicating that the copolymers have microphase-separated. More direct SAXS and T_g evidence is presented later. Since one of the blocks of the PTHF-*b*-PMMA copolymer is crystallizable when cast from solution, in general the copolymer can both microphase-separate and crystallize. Our d.s.c. study on the PTHF homopolymer showed that on cooling its crystallization temperature (T_c) was ca. 284 K, and its isothermal crystallization at 288 K was completed in just a few minutes. When cast from $CHCl_3$ at 288 K, the PTHF homopolymer formed well-developed spherulites as soon as the bulk film was formed. However, when the PTHF-*b*-PMMA diblock copolymers were cast from the same, non-selective solvent $CHCl_3$, again at 288 K, they did not crystallize at all during the first 2 h; this included copolymers L-6 and H-7 (*Table 1*) where the PTHF weight fractions are 0.61 and 0.65, respectively. *Figure 1* is the SAXS curve of the copolymer L-5 (*Table 1*), measured as soon as the cast film was dry. WAXD measurements of the same copolymer sample and its corresponding PTHF prepolymer were carried out immediately after the SAXS measurements (*Figures 2a* and *2b*). Since the WAXD patterns showed that the copolymer did not crystallize, while the homopolymer did, the SAXS peak in *Figure 1* represents only the contribution of the microphase separation of the copolymer initiated by the incompatibility of the two different blocks; this was also confirmed by the unchanged SAXS curve measured at a higher temperature than the melting point of the PTHF homopolymer. In fact, the copolymer can only crystallize slowly in the formed PTHF microphase at room temperature because the nucleation is very difficult, as shown in *Figures 2c* and *2d*, where the crystalline WAXD patterns of the L-5 and H-4 copolymers are presented after they had crystallized at 288 K for 3 weeks. This

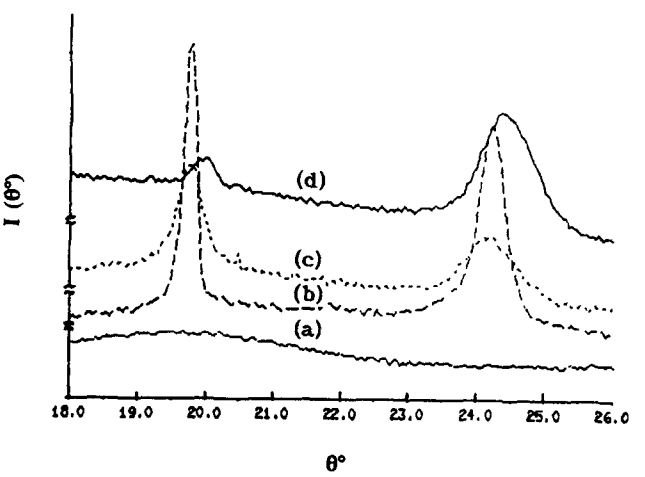

Figure 2 The WAXD patterns of the PTHF-*b*-PMMA copolymer L-5 (a) and the PTHF homopolymer L-7 (b), measured immediately after they had been cast from $CHCl_3$, plus the patterns of the copolymer samples L-5 (c) and H-4 (d), measured after they had slowly crystallized at 288 K for 3 weeks

shows that when the PTHF-*b*-PMMA diblock copolymers were cast from solution microphase separation and crystallization takes place separately; the microphase separation occurs first, and then the crystallization starts gradually, even for the copolymers where the major component is PTHF, such as L-6 and H-7.

Non-isothermal crystallization kinetics

Figure 3 shows that the crystallization temperature T_c of the PTHF-*b*-PMMA copolymers decreases greatly with increases in the amorphous PMMA weight fraction. The lowest T_c of the PTHF-*b*-PMMA copolymer is ca. 35 K lower than the T_c of the PTHF homopolymer. This indicates that the higher the PMMA content, then the lower the nucleation and crystallization rate of the PTHF-*b*-PMMA copolymer. As also shown in *Figure 3*, there is a clear T_c dependence on the molecular weight of

the PTHF block; at a given copolymer composition, the T_c of the copolymer with a PTHF block of $\bar{M}_n = 5100$ is obviously lower than that of the copolymer with the longer PTHF block ($\bar{M}_n = 7000$). When the PTHF weight fraction decreases to a certain critical value, no crystallization could be detected by d.s.c. on cooling; these critical fractions are 0.3 and 0.15 for the L- and H-series of copolymers, respectively, indicating that when the molecular weight of the PTHF block is higher, then a smaller PTHF weight fraction is needed for the copolymer to be able to crystallize in the PTHF microphase. Since the microphase separation of the copolymer takes place well in advance of its crystallization when it is cast from solution at room temperature, the dependence of its microdomain morphology on the composition, and the dependence of its microdomains size on the molecular weight are similar to that of an amorphous diblock copolymer, i.e. the above T_c dependence on the molecular weight of the PTHF block is essentially the dependence of its crystallizability on the PTHF microdomain size. The larger the PTHF domains, then the easier is the crystallization.

Figure 3 also showed that there is a big difference between the crystallization of the PTHF-*b*-PMMA diblock copolymers and the PTHF/PMMA blends. Unlike the copolymer, the crystallization temperatures of the blends do not decrease with increases in the PMMA content; instead, they increase slightly, probably due to the nucleation role of the interface of the macroscopic separated phases.

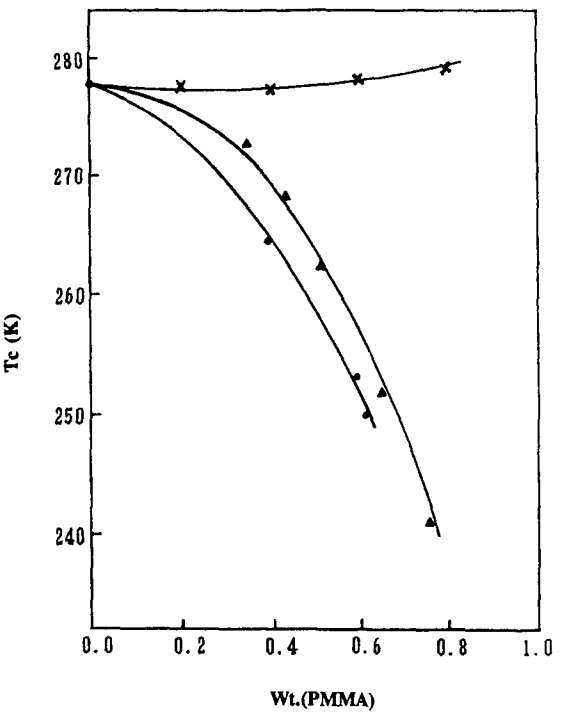

Figure 3 The curves of the crystallization temperature (T_c) of various samples on cooling, plotted as a function of the PMMA weight fraction: (×) PMMA/PTHF blends; (●) L- and (▲) H- series of PMMA-*b*-PTHF diblock copolymers

Melting behaviour and crystallinity of PTHF microphase

Figure 4 shows the melting point (T_m) dependence of the PTHF-*b*-PMMA copolymers and the PTHF/PMMA blends on the PMMA weight fraction; the melting point data were obtained on reheating the samples. As shown in *Figure 4*, the T_ms of the copolymers decrease rapidly with increases in the MMA weight fraction; the lowest T_m of the PTHF-*b*-PMMA copolymer is ca. 15 K lower than the T_m of the PTHF homopolymer. The melting behaviour of the copolymers is also different from the PTHF/PMMA blends (*Figure 4*), where the T_ms of the latter decreased very little with increases in the PMMA weight fraction. *Figure 4* also showed that at a given copolymer composition, the PTHF-*b*-PMMA copolymer with the shorter crystallizable block had a lower T_m, with this difference becoming larger for the copolymers whose major component is PMMA. Since the domain size is dependent on the molecular weight of the PTHF block, therefore the above T_m dependence on the molecular weight of the PTHF block is also essentially a dependence on the PTHF domain size.

The enthalpy of fusion of PTHF, $\Delta H_m^\circ = 12.4\,\mathrm{kJ\,mol^{-1}}$ (ref. 41), i.e. $\Delta H_m^\circ = 172.22\,\mathrm{J\,g^{-1}}$, was used to calculate the degree of crystallinity X_c of each PTHF microphase. *Figure 5* gives the X_c curve plotted as a function of the PMMA weight fraction. It can be found from this figure that the measured X_c decreases rapidly as the PMMA weight fraction increases, indicating that the very small size of the PTHF microphase, the 'joint' between the crystallizable PTHF block and the PMMA block, and the conformational constraint of the PTHF blocks in its microphase greatly restricted the crystallinity. The X_c depression with the increase in

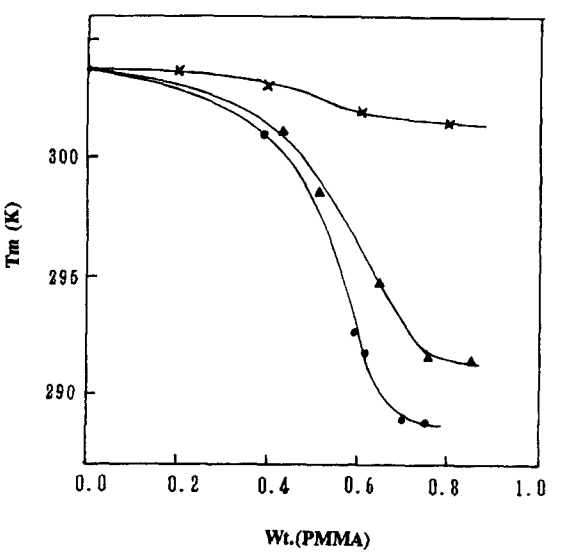

Figure 4 The melting point (T_m) curves of various samples plotted as a function of PMMA weight fraction: (×) PMMA/PTHF blends; (●) L- and (▲) H- series of PMMA-*b*-PTHF diblock copolymers.

PMMA weight fraction could also partly result from the surface-to-volume ratio of the PTHF microphases.

Although no crystallization peaks were observed for the L-1, L-2, L-3 and H1 samples on cooling (*Figure 3*), melting peaks were observed for L3 and H1 samples on subsequent heating. However, no melting peaks were observed for samples L1 and L2, whose PTHF weight fractions are 0.21 and 0.25, respectively, indicating that they were not able to crystallize at all. Since the crystallinity X_c of the PTHF homopolymer with low molecular weight is obviously higher than that of the PTHF homopolymer with high molecular weight[41] (*Figure 5*), at any copolymer composition with a PTHF

weight fraction PTHF ≥ 0.35, the X_c of the PTHF block of the copolymer with short PTHF blocks is still higher than that of the copolymer with long PTHF blocks. However, when the PTHF weight fraction is less than 0.35, i.e. when dispersed PTHF domains are supposed to be formed, the copolymer with short PTHF blocks has a lower X_c than that of the copolymer with the longer PTHF blocks, as shown in *Figure 5*, thus suggesting that the larger the size of the dispersed PTHF domain, then the stronger the crystallizability and the higher the crystallinity will be.

The glass transition

Differential scanning calorimetry was used to study the glass transition temperatures, T_gs, of the PTHF-*b*-PMMA diblock copolymers. Since both the H- and L-series of copolymers have their own given lengths of PTHF blocks but different lengths of PMMA blocks (*Table 1*), it is very convenient to study the T_g dependence of the PMMA microphase on the molecular weight of the PMMA block at a given length of PTHF block. As shown in *Table 2*, the T_g of the PMMA microphase of both the H- and L-series of copolymers decrease with decreasing molecular weight of the PMMA block. The higher T_g of the PMMA microphase in sample H-3 when compared to that in sample L-3 (*Table 2*), where both have the same H-3 composition but with a shorter PMMA block for the latter, gives further evidence of the T_g dependence of the PMMA microphase on the molecular weight of the block. A T_g corresponding to the PMMA microdomains in sample L-6 was not observed, probably due to the very small molecular weight of the copolymer ($M_n = 8400$) and hence the small degree of incompatibility of the two blocks.

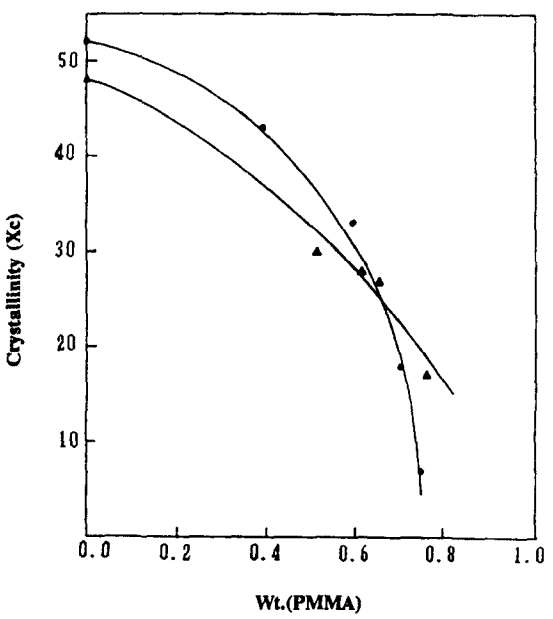

Figure 5 The crystallinity degree curves of the (●) L- and (▲) H-series of PTHF-*b*-PMMA diblock copolymers plotted as a function of the PMMA weight fraction

Since both the H- and L-series of PTHF-*b*-PMMA diblock copolymers have their own given PTHF length but different PMMA lengths, this also made it possible to study the T_g dependence of the PTHF microphase on the copolymer composition. In our experiments, the glass transition of the PTHF microdomains could only be observed for samples with a PTHF weight fraction ≥ 0.35. As shown in *Table 2*, the T_g of the PTHF microphase of the L-series samples increases with increasing the PTHF weight fraction, i.e. the T_g changes with copolymer composition. Another feature of the T_g of the PTHF microphase is that the T_g values listed in *Table 2* are much higher than the T_g of the PTHF homopolymer[41] and the PTHF microphases in PTHF/PS di- or triblock copolymer reported in literature[24]. There is a general agreement that PTHF forms a glass at about 187 K; low-molecular-weight glycols may do so at a somewhat higher temperature[41]. The reported highest T_g of PTHF was about 210 K[24,41]. Therefore, the T_gs of PTHF microphases obtained in the present study on PTHF-*b*-PMMA copolymers are about 30 K higher than the reported highest T_g values.

The same conclusion that the higher the molecular weight of the amorphous block, the higher the T_g of its corresponding microphase, was also achieved by Takahashi and Yamashita[24] for PTHF/PS di- and triblock copolymers, and by Crystal, Erhardt and O'Malley[43,44] for PEO-*b*-PS diblock copolymers. But Takahashi and Yamashita's results did not show any T_g dependence of PTHF microphase on copolymer composition, or on the molecular weight of PTHF block, although the number average molecular weights of PTHF blocks of their copolymers ranged from 60 500 to 134 000; their dynamic

Table 2 The glass transition temperatures of the PMMA and PTHF microdomains of PTHF-*b*-PMMA diblock copolymers

	PTHF block		PMMA block	T_g (K)	
Designation	M_n	Wt%	M_n	PMMA domains	PTHF domains
H-0	0	0	20 000	378	–
H-2	7000	24	22 170	375	–
H-3	7000	30	16 300	373	–
H-4	7000	35	13 000	369	238
L-1	5100	21	19 200	372	–
L-3	5100	30	11 900	369	–
L-4	5100	39	8000	357	234
L-5	5100	41	7340	352	238
L-6	5100	61	3260	–	242
L-7	5100	100	0	–	210[a]

[a] Represents the highest T_g of PTHF reported in the literature

mechanical measurements revealed that the T_g of PTHF microphase was about 209 K for all their samples. This difference probably came from the difference in the molecular weight range of the PTHF blocks of the PTHF/PS copolymers were about ten times higher than those of our PTHF-*b*-PMMA copolymers. However, the T_g dependence of a semicrystalline microphase on copolymer composition was found for dimethylsiloxane–styrene diblock copolymers (PDMS-*b*-PS) by Wang and Krause[25]. Their d.s.c. studies showed that for the copolymers having $\geq$40 wt% PDMS, the higher the PDMS content in the copolymer is, the higher the T_g of PDMS semicrystalline microphase is. Their theoretical calculation confirmed that this T_g increase was attributed to the effects of thermal stress field, which is caused by the unequal coefficients of thermal expansion of the two phases below the T_g of the PS microphase. The conclusion that the T_g of the semicrystalline microphase increases with increasing weight fraction of the crystallizable block was achieved both for the PDMS-*b*-PS and the PTHF-*b*-PMMA diblock copolymers. This similarity probably resulted from the final microphase morphology of these two copolymers being driven by microphase separation when cast from solution. Therefore, the microphases formed are not favourable for crystallization, and after they had partly and slowly crystallized, the PDMS and PTHF segments which failed to crystallize could adopt special conformations.

DISCUSSION

By comparison of the microphase separation and crystallization of PTHF-*b*-PMMA copolymers with those of PEO-*b*-PS copolymers, where the latter have been extensively reported in the literature, the following different features have been noted. First, in the case of solution-cast samples the microphase separation of the PTHF-*b*-PMMA copolymers takes place first, and then crystallization starts gradually, while microphase separation and crystallization of PEO-*b*-PS copolymers take place simultaneously with the final structure and morphology being driven by the balance between the two processes. Secondly, the non-isothermal crystallization kinetics of the PTHF-*b*-PMMA copolymers is very different from that of the PEO-*b*-PS copolymers. The T_c of the PTHF-*b*-PMMA copolymers decreases continuously and very rapidly with the increase in amorphous PMMA weight fraction; the lowest T_c found is ca. 35 K lower than that of the PTHF homopolymer, as shown in *Figure 3*. Poly(ethylene oxide) (PEO)-*b*-PS copolymers, however, behave similarly to the PEO homopolymer when the major component is PEO, and the T_c does not change much with composition. When the major component of the PEO-*b*-PS copolymers is PS, however, two distinct crystallization peaks, about 60 K apart, are observed, but the higher T_c is still near the T_c of the PEO homopolymer (ca. 315 K)[22]. This dual crystallization process becomes more evident in PEO–PS–PEO triblock copolymers. Since the T_g of the amorphous PMMA hard block is nearly the same as that of the PS block, and the degree of incompatibility between both PTHF and PMMA and between PS and PEO is very big, the above differences between the PTHF-*b*-PMMA and PEO-*b*-PS copolymers most likely result from the different nature of their crystallizable blocks.

The effect of block crystallizability on microphase separation and crystallization

High-molecular-weight PTHF is an excellent rubber, and such amorphous polymers possess an excellent green strength and good tack. The polymers with intermediate or low molecular weights can crystallize, but this crystallizability is easily weaken by copolymerization. Hence this polymer is widely used industrially as the soft segments in thermoplastic elastomers, e.g. polyurethane and polyester elastomers, where its tendency to crystallize slowly at room temperature is easily overcome[41]. The remarkable decrease of the non-isothermal crystallization temperature (T_c) of PTHF-*b*-PMMA diblock copolymers with increases in the PMMA weight fractions also largely results from the copolymerization.

Although PTHF and PEO are very similar in their molecular structure, our d.s.c. investigations show that for intermediate degrees of polymerization, PEO and PTHF crystallize at 315 and 277 K, respectively, during cooling at a given rate of 10 K min^{-1}, indicating that the nucleation, and hence the crystallization rate, of the PEO homopolymer is much higher than that of the PTHF homopolymer. The same conclusion was also reached by infra-red spectroscopic studies[41]. The weak ability for PTHF to crystallize means that when a PTHF-*b*-PMMA copolymer is cast from solution microphase separation takes place first and then the copolymer starts to gradually crystallize. The microphase-separation structure which is formed makes the crystallization of PTHF-*b*-PMMA diblock copolymers very difficult; this also includes melt crystallization. In contrast, in the case of the PEO-*b*-PS diblock copolymers, when cast from solution the final morphology is driven both by microphase separation (initiated by the incompatibility of the two blocks) and by crystallization. A third case was recently reported[36] in which the final morphology of a hydrogenated 1,4-butadiene–1,4-isoprene diblock copolymer only resulted from the crystallization process. We can therefore say that block crystallizability in semicrystalline–amorphous diblock copolymers is one of the key factors governing its final equilibrium morphology. The final morphology can only be driven either by crystallization or microphase separation, or by a balance between the two processes.

CONCLUSIONS

1. In the case of solution-cast samples, of PTHF-*b*-PMMA copolymers microphase separation takes place first and then crystallization gradually starts in the formed PTHF microphase. This is different to PEO-*b*-PS copolymers where both microphase separation and crystallization take place simultaneously, and is also different to hydrogenated 1,4-butadiene–1,4-isoprene diblock copolymers where the final morphology is only driven by crystallization.
2. The non-isothermal crystallization temperature (T_c) of the crystallizable block in PTHF-*b*-PMMA diblock copolymers decreases rapidly and continuously with increases in the amorphous MMA weight fraction; the lowest T_c of these PTHF-*b*-PMMA copolymer is ca. 35 K lower than the T_c of the PTHF homopolymer. This is similar to other miscible homopolymer blends (e.g. PEO/PMMA), but very different to PEO-*b*-PS diblock copolymers, which either have one T_c which is

slightly lower than that of the PEO homopolymer, or have two distinct crystallization peaks (ca. 60 K apart), depending on the copolymer composition.

3. There is also a T_c dependence on the molecular weight of the PTHF block at a given copolymer composition, with the higher molecular weights giving higher values for the T_c.
4. The degree of crystallinity of the PTHF microphase of the copolymer shows a large decrease with increases in the PMMA weight fraction, due to the change in the PTHF microphase morphology from a matrix phase to a final smaller dispersed microphase, and from the increase of the surface-to-volume ratio of the microphases.
5. The melting temperatures of the PTHF-*b*-PMMA block copolymers showed a strong dependence on the copolymer composition and on the molecular weight of its crystallizable block. This is very different from reports in the literature on PTHF/PS di- and triblock copolymers, where the T_m was almost independent of the copolymer composition[24]. This difference resulted from the large differences between the molecular weights of the PTHF blocks in the PTHF/PS and PTHF/PMMA block copolymers.
6. The T_g of the PMMA microphase showed a strong dependence on the molecular weight of the PMMA block, while the T_g of the PTHF microphase showed a strong dependence on the copolymer composition. This latter dependence was not previously reported in published studies on PTHF/PS di- and triblock copolymers with much higher molecular weights.

ACKNOWLEDGEMENT

This work was supported by the National Basic Research Project, 'The Macromolecular Condensed State'.

REFERENCES

1 Leibler, L. *Macromolecules* 1980, **13,** 1602
2 Leibler, L. *Macromolecules* 1982, **15,** 1283
3 Helfand, E. *Macromolecules* 1975, **8,** 552
4 Helfand, E and Wasserman, Z. *Macromolecules* 1976, **9,** 879
5 Helfand, E. and Wasserman, Z. *Macromolecules* 1978, **11,** 960
6 Helfand, E. and Wasserman, Z. *Macromolecules* 1980, **13,** 994
7 Kawasaki, K., Ohta, T. and Kohrogui, M. *Macromolecules* 1988, **21,** 2972
8 Semenov, M. N. *Macromolecules* 1989, **22,** 2849
9 Thomas, E. L., Alward, D. B., Kinning, D. J., Martin, D. C., Handlin, D. L. and Fetters, L. J. *Macromolecules* 1986, **19,** 2197
10 Hasegawa, H., Tanaka, H. Yamasaki, K. and Hashimoato, T. *Macromolecules* 1987, **20,** 1651
11 Thomas, E. L., Kinning, D. J., Alward, D. B. and Henkee, C. S. *Macromolecules* 1987, **20,** 2934
12 Roe, R. J., Fishkis, M. and Chang, V. C. *Macromolecules* 1981, **14,** 1091
13 Richards, R. W. and Thomason, J. L. *Macromolecules* 1983, **16,** 982
14 Ohta, T. and Kawasaki, K. *Macromolecules* 1986, **19,** 2621
15 Hashimoto, T. *Macromolecules* 1987, **20,** 468
16 Winey, K. I.. Patel, S. S., Larson, R. G. and Watanabe, H. *Macromolecules* 1993, **26,** 2542
17 Gervais, M. and Gallot, B. *Makromol. Chem.* 1973, **171,** 157
18 Gervais, M. and Gallot, B. *Makromol. Chem.* 1973, **174,** 193
19 Gervais, M. and Gallot, B. *Makromol. Chem.* 1977, **178,** 2071
20 Gervais, M. and Gallot, B. *Polymer* 1981, **22,** 1129
21 Gast, A. P., Vinson, P. K. and Cogan-Farinas, K. A. *Macromolecules* 1993, **26,** 1774
22 O'Malley, J. J. *J. Polym. Sci. Polym. Symp.* 1977, **60,** 151
23 Short, J. M. and Crystal, R. G. *Appl. Polym. Symp.* 1971, **16,** 137
24 Takahashi, A. and Yamashita, Y. in 'Copolymers, Polyblends and Composites Symp., 1974' (Ed. A. J. Platzer), ACS Advances in Chemistry Series, Vol. 142, American Chemical Society, Washington, DC, 1975, p. 267
25 Wang, B. and Krause, S. *Macromolecules* 1987, **20,** 2201
26 Heuschen, J., Vion, J. M., Jerome, R. and Teyssie, Ph. *Macromolecules* 1989, **22,** 2446
27 Chow, T. S. *Macromolecules* 1990, **23,** 333
28 Veith, C. A., Cohen, R. E. and Argon, A. S. *Polymer* 1991, **32,** 1545
29 Douzinas, K. C., Cohen, R. E. and Halasa, A. F. *Macromolecules* 1991, **24,** 4457
30 Douzinas, K. C. and Cohen, R. E. *Macromolecules* 1992, **25,** 5030
31 Nojima, S., Kato, K., Yamamoto, S. and Ashida, T. *Macromolecules* 1992, **25,** 2237
32 Ishikawa, S., Sasaki, S. and Fukutomi, T. J. *Appl. Polym. Sci.* 1993, **48,** 509
33 Cohen, R. E., Cheng, P. L., Douzinas, K. C., Kofinas, P. and Berney, C. V. S. *Macromolecules* 1990, **23,** 324
34 Ishikawa, S. and Fukutomi, T. *Eur. Polym. J.* 1993, **29,** 877
35 Limtasiri, T., Grossman, S. J. and Huang, J. C. *Polym. Eng. Sci.* 1989, **29,** 493
36 Rangarajan, P., Register, R. A. and Fetters, L. J. *Macromolecules* 1993, **26,** 4640
37 Whitmore, M. D. and Noolandi, J. *Macromolecules* 1988, **21,** 1482
38 Dimarzio, E. A., Guttman, C. M. and Hoffman, J. D. *Macromolecules* 1980, **13,** 1194
39 Vilgis, T. and Halperin, A. *Macromolecules* 1991, **24,** 2090
40 Chow, T. S. *Macromolecules* 1981, **14,** 1386
41 Dreyfuss, P. 'Poly(tetrahydrofuran)', Gordon and Breach, New York, 1982
42 Liu, L-Z. *PhD Thesis*, Changchun Institute of Applied Chemistry, People's Republic of China, 1992
43 Crystal, R. G., Erhardt, P. F. and O'Malley, J. J. in 'Block Copolymers' (Ed. S. L. Aggarwal), Plenum, New York, 1970, p. 179
44 O'Malley, J. J., Crystal, R. G. and Erhardt, P. F. in 'Block Copolymers' (Ed. S. L. Aggarwal), Plenum, New York, 1970, p. 163